# Complex Interactions of Carbon Monoxide with Reduced Cytochrome *cbb*$_3$ Oxidase from *Pseudomonas stutzeri*†

Robert S. Pitcher,‡ Thomas Brittain,§ and Nicholas J. Watmough*,‡

*Centre for Metalloprotein Spectroscopy and Biology, School of Biological Sciences, University of East Anglia, Norfolk NR4 7TJ, United Kingdom, and School of Biological Sciences, University of Auckland, Private Bag 92019, Auckland, New Zealand*

*Received March 3, 2003; Revised Manuscript Received August 6, 2003*

ABSTRACT: Cytochrome *cbb*$_3$ oxidase, from *Pseudomonas stutzeri*, contains a total of five hemes, two of which, a *b*-type heme in the active site and a hexacoordinate *c*-type heme, can bind CO in the reduced state. By comparing the *cbb*$_3$ oxidase complex and the isolated CcoP subunit, which contains the ligand binding bishistidine-coordinated *c*-type heme, we have deconvoluted the contribution made by each center to CO binding. A combination of rapid mixing and flash photolysis experiments, coupled with computer simulations, reveals the kinetics of the reaction of *c*-type heme with CO to be complex as a result of the need to displace an endogenous axial ligand, a property shared with nonsymbiotic plant hemoglobins and some heme-based gas sensing domains. The recombination of CO with heme $b_3$, unlike all other heme−copper oxidases, including mitochondrial cytochrome *c* oxidase, is independent of ligand concentration. This observation suggests a very differently organized dinuclear center in which CO exchange between $Cu_B$ and heme $b_3$ is significantly enhanced, perhaps reflecting an important determinant of substrate affinity.

Cytochrome *cbb*$_3$ oxidase is a bacterial respiratory enzyme that catalyzes the four-electron reduction of dioxygen to water. The *cbb*$_3$-type heme−copper oxidases (HCOs)[1] are members of the same superfamily of enzymes that includes cytochrome *aa*$_3$ (mitochondrial cytochrome *c* oxidase), the bacterial quinol oxidase cytochrome *bo*$_3$, and the bacterial nitric oxide reductase (NOR) (*1*, *2*). What appears to distinguish cytochromes *cbb*$_3$ from the other proton-motive terminal oxidases of the HCO superfamily is the very high affinity for oxygen ($K_m \sim 7$ nM) that has been reported for the enzyme isolated from *Bradyrhizobium japonicum* (*3*). This property, coupled with an ability to conserve energy in the form of a proton gradient (*4*), is likely to be important to the proposed role of these distinctive oxidases in allowing bacteria to colonize anoxic environments (*5*).

Cytochrome *cbb*$_3$ is encoded by the *ccoNOQP* operon (*6*, *7*), but is usually purified as a three-subunit complex CcoNOP (*8*). The catalytic subunit, CcoN, which is homologous to subunit I of other HCOs contains the active site. This is a dinuclear center composed of a high-spin *b*-type heme, known as heme $b_3$,[2] magnetically coupled to a nearby copper ion ($Cu_B$). A second, magnetically isolated, low-spin *b*-type heme in the CcoN subunit is responsible for transferring electrons to the active site. There is considerable interest in the catalytic subunit of *cbb*$_3$-type oxidases, because many of the residues that have been shown to be essential for proton movements during turnover of cytochrome *aa*$_3$ are not conserved in the derived amino acid sequences of CcoN (*7*, *9*). The absence of these residues together with the presence of a *b*-type heme, which lacks the hydroxyethylfarnesyl side chain of Heme O and Heme A, in the dinuclear center may influence the substrate binding properties of the *cbb*$_3$-type oxidases.

Although cytochrome *cbb*$_3$ receives its substrate electrons from the cytochrome *bc*$_1$ complex via cytochrome *c*, it has no $Cu_A$ center in its electron-receiving domain. Instead, this role is fulfilled by one of two membrane-anchored subunits, CcoO and CcoP, which contain one and two *c*-type hemes, respectively. There is some evidence that subcomplexes containing only CcoN and CcoO are catalytically competent (*9*, *10*), leaving some uncertainty about the role of, or requirement for, CcoP. We have recently completed a detailed biochemical and spectroscopic analysis of the cytochrome *cbb*$_3$ oxidase purified from *Pseudomonas stutzeri* in which we demonstrated that CcoP contains a bishistidine-coordinated *c*-type heme (*8*). A subsequent spectro-electro-

† Supported by grants from the Wellcome Trust (054798/Z/98/Z and 066363/Z/01/Z) and a studentship from the UK Biotechnology and Biological Sciences Research Council (99/A1/C/05140).

* To whom correspondence should be addressed. Telephone: +44 (1603) 592179. Fax: +44 (1603) 592250. E-mail: n.watmough@uea.ac.uk.

‡ University of East Anglia.

§ University of Auckland.

[1] Abbreviations: DM, dodecyl β-D-maltoside; *Ec*Dos, *Escherichia coli* direct oxygen sensor; FTIR, Fourier transform infrared; HCO, heme−copper oxidase; NOR, nitric oxide reductase; NIR-MCD, near-infrared magnetic circular dichroism; SHP, *sphaeroides* heme protein.

[2] To aid comparison with other heme−copper oxidases, we have adopted the following notation for the metal centers in CcoN which is structurally related to cytochrome *c* oxidase (cytochrome *aa*$_3$) subunit I. Heme *b* is the low-spin bishistidine-coordinated heme in CcoN that is a homologue of heme *a* in cytochrome *c* oxidase. Heme $b_3$ is high-spin in CcoN and equivalent to heme $a_3$ in cytochrome *c* oxidase and heme $o_3$ of *E. coli* cytochrome *bo*$_3$ quinol oxidase. In cytochrome *c* oxidase and quinol oxidases, this heme is magnetically coupled to a copper ion ($Cu_B$) to form a dinuclear center which is the site of oxygen binding and reduction. $Cu_B$ in CcoN is probably ligated by three conserved histidine residues, which also serve as ligands to $Cu_B$ in cytochrome *c* oxidase.

10.1021/bi0343469 CCC: $25.00 
Published on Web 09/06/2003

chemical analysis showed that the potential of this heme, although relatively low ($E^{\circ\prime} = 185$ mV), does not exclude a role for CcoP in electron transfer into the complex (*11*).

Reduced hemes often bind carbon monoxide (CO), a diatomic gas that is a substrate analogue of oxygen. The binding of CO induces marked spectroscopic changes in the absorption spectrum of the ferrous heme and thus provides a convenient method for distinguishing between those hemes in which the sixth ligand is absent (pentacoordinate species) or can be displaced by CO and those hemes in which both axial ligands are stable (*12*). The complex that is formed contains an Fe(II)−CO bond that is photolabile. Transient illumination causes this bond to break, an event which is followed by CO recombination to the now pentacoordinate ferrous heme. The kinetics of such CO recombination events are a very sensitive probe of the environment of the oxygen binding heme that has been applied to a number of proteins, including both globins and HCOs (*13*, *14*).

The rate of recombination of CO to the reduced active site heme of HCOs ($7 \times 10^4$ $M^{-1}$ $s^{-1}$) (*13*) is significantly slower than the rate of recombination to myoglobin ($5 \times 10^5$ $M^{-1}$ $s^{-1}$) (*14*) because of the photolyzed CO interacting with the reduced $Cu_B$. The transient ligation of CO at another site is reflected in saturating recombination kinetics at concentrations above 10 mM in bovine mitochondrial cytochrome *c* oxidase (*15*) and cytochrome $bo_3$ oxidase from *Escherichia coli* (*16*). The intermediate species, $Cu_B$−CO, has been directly observed by low-temperature FTIR spectroscopy and is diagnostic of the heme−copper dinuclear center (*17*). Consequently, those forms of cytochrome $bo_3$ that lack $Cu_B$ in the dinuclear center exhibit a rate of CO recombination that is higher ($k_{on} = 2-4 \times 10^5$ $M^{-1}$ $s^{-1}$) than that of copper replete cytochrome $bo_3$ and proportional to the concentration of CO over the range of 0−20 mM (*16*). In bacterial NOR, the rate of CO recombination to the reduced active site heme is 4 orders of magnitude greater ($1.7 \times 10^8$ $M^{-1}$ $s^{-1}$) than that seen in other HCOs (*18*). This is presumably because after photolysis CO does not interact with non-heme iron that replaces $Cu_B$ in the dinuclear center of NOR (*19*).

Investigating the kinetics of CO recombination to the active site heme of a cytochrome $cbb_3$ oxidase would give new information about the organization of the dinuclear center. In addition, it is a necessary prelude to other experiments in which CO-bound forms of the enzyme are used as a starting point to assess internal electron transfer (*20*) and a single turnover of the reduced enzyme with oxygen (*13*). Unfortunately, these initial experiments have been complicated by evidence of heterogeneous binding of CO to the hemes of cytochromes $cbb_3$. For example, the enzyme isolated from *B. japonicum* apparently binds CO to both *b*- and *c*-type cytochromes (*3*, *21*).

In this paper, we report a detailed study of the interaction of reduced cytochrome $cbb_3$ oxidase from *P. stutzeri* with CO using flash photolysis and rapid mixing kinetics. This enzyme exhibits a complex pattern of interaction with CO, but by comparing the kinetics of CO recombination to the holoenzyme with the isolated heme *c* containing subunit CcoP, we have been able to deconvolute the contribution made by each center and comment on the possible significance of their quite different CO binding properties.

## MATERIALS AND METHODS

*Growth Conditions and Protein Purification.* Methods for the batch culture of *P. stutzeri* ZoBell (ATCC 14405) and *E. coli* JM109 (DE3), transformed with pCcoPall and pEC86, and the subsequent purification of cytochrome $cbb_3$ oxidase from *P. stutzeri* and recombinant CcoP from *E. coli* were as previously described (*8*). The purity of cytochrome $cbb_3$ oxidase (>95%) and CcoP (>99%) was assessed by SDS−PAGE and a combination of UV−vis and EPR spectroscopies. The heme content of the purified proteins was determined using the pyridine hemochromogen method (*22*). Purified proteins were stored in aliquots at −80 °C until they were needed.

*Spectroscopy.* Electronic absorption spectra (UV−vis) were recorded under strictly anaerobic conditions using a Hitachi U3100 spectrophotometer as previously described (*8*). The concentrations of oxidized cytochrome $cbb_3$ and CcoP were calculated on the basis of their molar extinction coefficients: $\epsilon_{411} = 5.85 \times 10^5$ $M^{-1}$ $cm^{-1}$ and $\epsilon_{408} = 2.7 \times 10^5$ $M^{-1}$ $cm^{-1}$, respectively (*8*). Reduction of the purified proteins was achieved by either the addition of small aliquots of sodium dithionite (final concentration of ∼50 $\mu$M) or sodium ascorbate (final concentration of 1 mM).

The reduced CO adduct was prepared by two different methods depending on the final concentration of CO in solution. When low final concentrations of CO were required (≤100 $\mu$M), small aliquots of CO-saturated buffer [20 mM sodium phosphate, 50 $\mu$M EDTA, and 0.02% (w/v) DM (pH 7.5)] were added to an anaerobic cuvette containing reduced protein using a gastight syringe. When higher final concentrations were required, appropriate mixtures of oxygen free buffer [20 mM sodium phosphate, 50 $\mu$M EDTA, and 0.02% (w/v) DM (pH 7.5)] prepared in an anaerobic cabinet and CO-saturated solutions of the same buffer (total volume of ∼3.9 mL) were added as appropriate to a small volume (<150 $\mu$L) of concentrated reduced protein in a sealed anaerobic cuvette prepared as described above.

*Optically Monitored Titrations of CO Binding.* Titrations with CO were monitored spectroscopically after successive additions of small aliquots of CO-saturated buffer to a sealed cuvette filled completely with either a solution of fully reduced CcoP or cytochrome $cbb_3$ oxidase. A small magnetic stirrer was added to the cuvette to facilitate mixing. Anaerobic conditions were maintained by using gastight syringes for all additions of CO, and a small aliquot of a sodium dithionite solution was added to the CO-saturated buffer to remove any traces of oxygen.

*Kinetic Measurements.* The recombination of CO with fully reduced cytochrome $cbb_3$ oxidase (1−3 $\mu$M) and CcoP (1−5 $\mu$M) over a range of CO concentrations (10 $\mu$M to 1 mM, prepared as outlined above) was assessed using an LKS.50 laser kinetic spectrometer (Applied Photophysics, Leatherhead, U.K.). Photolysis of CO was initiated by a laser pulse (6 ns) generated by a frequency-doubled Nd:YAG laser (Spectron Laser Systems, Rugby, U.K.). The progress of reactions was monitored at single wavelengths between 400 and 450 nm and recorded using a Hewlett-Packard 54520A digitizing oscilloscope. At each wavelength, five to nine separate transients were acquired and the data averaged.

The reaction between fully reduced CcoP (1−3 $\mu$M) and CO was assessed in an Applied Photophysics Bio-Sequential

Scheme 1

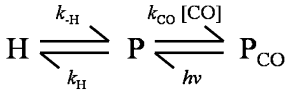


Scheme 2

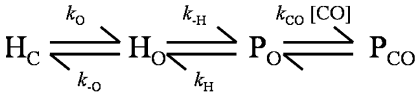


DX.17MV stopped-flow spectrophotometer, with a dead time of ~2 ms, using a 1 cm path length cell. At least 1000 data points were collected for each experiment with a split time base with a maximum time resolution of 0.2 ms. A minimum of five traces were collected at each concentration and the data averaged.

*Analysis of Kinetic Data.* All rapid reactions were performed under pseudo-first-order conditions, and reaction time courses were analyzed in terms of either single-exponential processes or the sum of exponential processes. All reactions were performed at 20 °C. All kinetic traces were exported as ASCII files and analyzed using Tablecurve 2D (Jandel Scientific). Spectra and fits were replotted in Origin version 4.1 (Microcal).

Our earlier work had indicated that both *c*-type hemes in CcoP were hexacoordinate in the ferric state (*8*). Consequently, kinetic data resulting from the postphotolysis recombination of CO with a single *c*-type heme in CcoP were fitted to a model developed by Hargrove to characterize CO recombination in plant hemoglobins that contain a hexacoordinated heme (*23*). After photolysis, the heme, which is initially six-coordinate ($P_{CO}$), becomes pentacoordinate (P) and can undergo two competing reactions, either forming the hexacoordinate form H or else recombining with the ligand to yield the initial CO-bound form ($P_{CO}$) (eq 1). An analytical solution for the time course for the production of $P_{CO}$ exists when the reaction proceeds from P (*24*).

$$[P_{CO}] = [P]_o\left\{1 - \left[\frac{k_{CO}[CO](k_{-H} - \gamma_1)}{\gamma_1(\gamma_2 - \gamma_1)}\right]e^{-\gamma_1 t} - \left[\frac{k_{CO}[CO](k_{-H} - \gamma_2)}{\gamma_2(\gamma_1 - \gamma_2)}\right]e^{-\gamma_2 t}\right\} \quad (1)$$

where the observed rate constant for the fast phase ($\gamma_1$) is described by

$$\gamma_1 = \frac{(k_H + k_{-H} + k_{CO}[CO]) + [(k_H + k_{-H} + k_{CO}[CO])^2 - 4k_{-H}k_{CO}[CO]]^{1/2}}{2} \quad (2)$$

and the observed rate constant for the slow phase ($\gamma_2$) is described by

$$\gamma_2 = \frac{k_H + k_{-H} + k_{CO}[CO] - [(k_H + k_{-H} + k_{CO}[CO])^2 - 4k_{-H}k_{CO}[CO]]^{1/2}}{2} \quad (3)$$

As Scheme 1 could not account for the kinetic complexity seen in the rapid mixing experiments, the reaction of reduced CcoP with CO after rapid mixing was analyzed using a model developed by Trent and colleagues to characterize the initial reaction of CO with the reduced heme of plant hemoglobin in rapid mixing experiments (Scheme 2) (*25*). In our experiments, and presumably under physiological conditions, the CO-binding *c*-type heme in CcoP would exist as an equilibrium mixture of hexacoordinate ($H_O$) and pentacoordinate ($P_O$) "open" forms that can bind CO. In addition there is a "closed" subpopulation of hexacoordinate heme ($H_C$) that is neither able to bind CO nor in rapid equilibrium with the ligand binding forms on the time scales of our experiments.

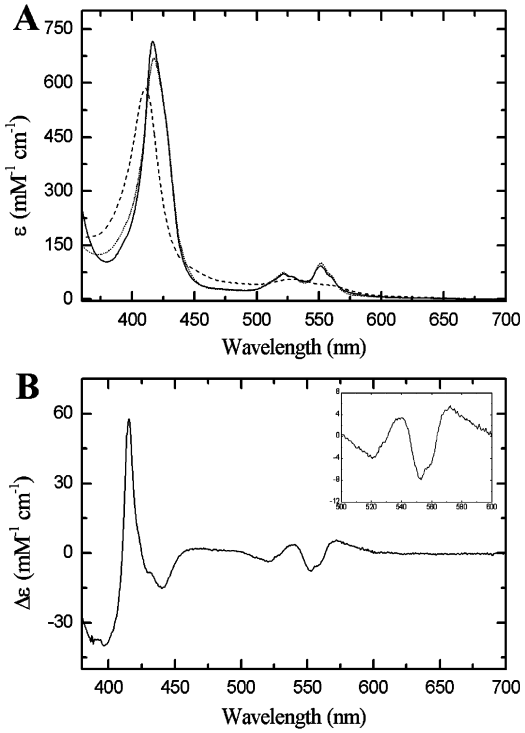


FIGURE 1: (A) Electronic absorption spectrum of cytochrome *cbb*$_3$ oxidase from *P. stutzeri* (1.5 $\mu$M) recorded at room temperature in 20 mM sodium phosphate, 50 $\mu$M EDTA, and 0.02% (w/v) DM (pH 7.5). The air-oxidized enzyme as purified (− − −) was fully reduced by the addition of excess sodium dithionite (···) before treatment with 1 mM CO (—). (B) Reduced-CO *minus* reduced difference spectrum calculated from the traces shown in panel A. The inset of panel B shows the region between 500 and 600 nm in detail.

Using steady-state approximations for $H_O$ and $P_O$, the observed rate constant ($k_{obs}$) for the formation of $P_{CO}$ following rapid mixing is described by eq 4. Note that the rate constants $k_{-H}$, $k_H$, and $k_{CO}$ in this expression are identical to those used in eqs 2 and 3.

$$k_{obs} = \frac{k_{-H}k_O k_{CO}[CO]}{k_H k_{-O} + k_O(k_{-H} + k_H) + (k_O + k_{-O} + k_{-H})k_{CO}[CO]} \quad (4)$$

## RESULTS

*Effect of CO Binding on the Electronic Absorption Spectrum of Cytochrome cbb*$_3$. The effect of CO binding to fully reduced cytochrome *cbb*$_3$ oxidase is readily seen in the electronic absorption spectrum (Figure 1A). The Soret band

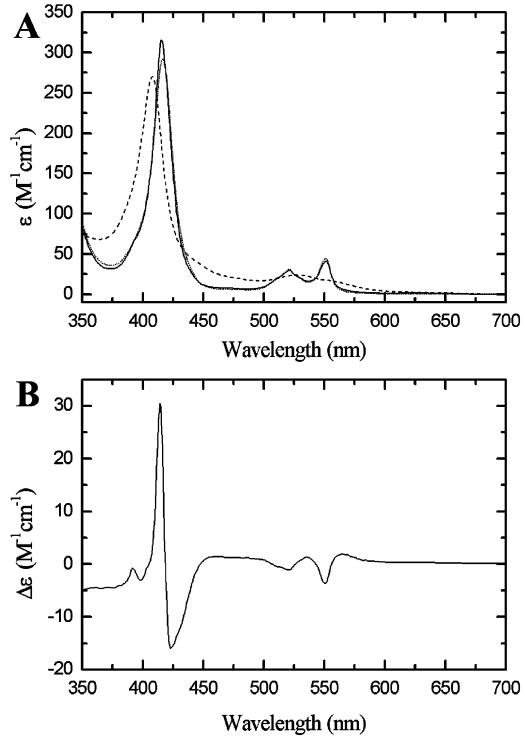


FIGURE 2: (A) Electronic absorption spectrum of recombinant *P. stutzeri* CcoP (5.7 $\mu$M) recorded at room temperature in 20 mM sodium phosphate, 50 $\mu$M EDTA, and 0.02% (w/v) DM (pH 7.5). The spectrum of the protein was recorded after oxidation with potassium ferricyanide (− − −). After the addition of excess sodium dithionite, the spectrum of the fully reduced protein was recorded (···), before treatment with 1 mM CO (—). (B) Reduced-CO *minus* reduced difference spectrum calculated from the traces shown in panel A.

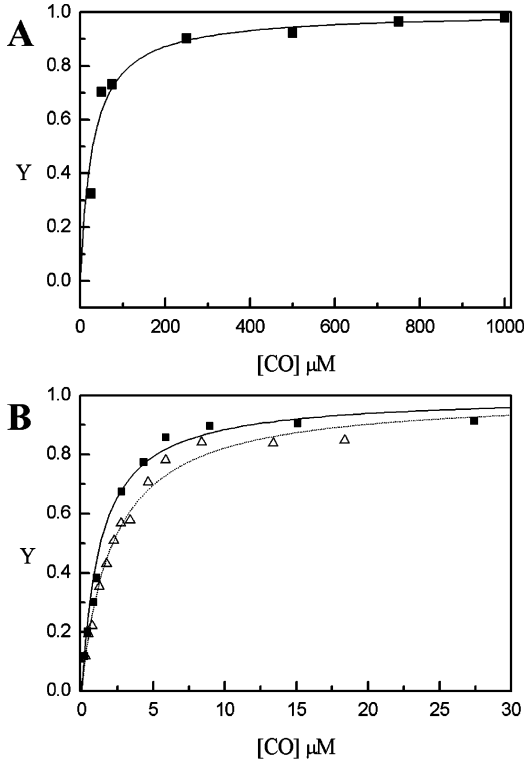


FIGURE 3: (A) Samples of fully reduced CcoP (2.4 $\mu$M) and cytochrome *cbb*$_3$ oxidase (4.5 $\mu$M) were made in 20 mM sodium phosphate, 50 $\mu$M EDTA, and 0.02% (w/v) DM (pH 7.5) in sealed cuvettes. The samples were titrated with CO at room temperature, and the resultant absorbance changes at 415 nm were used to calculate the fractional saturation (*Y*) of the ferrous *c*-type heme with CO. To obtain the dissociation constant for CO binding, the data obtained with CcoP (△) and cytochrome *cbb*$_3$ oxidase (■) were independently fitted using the function $Y = (K_D[CO])/(1 + K_D[CO])$, assuming that CO binds to only a single site. The fits are to the data obtained for cytochrome *cbb*$_3$ oxidase (—) and CcoP (···) are shown separately. (B) The total change in transient absorption at 424 nm associated with CO recombination to heme $b_3$ after photolysis was measured at a range of CO concentrations and used to calculate the fractional saturation (*Y*) of ferrous heme $b_3$ with CO. All transients were recorded at room temperature. The dissociation constant was calculated from the data using the function $Y = (K_D[CO])/(1 + K_D[CO])$, again making the assumption that CO binds to only a single site (—).

is at a slightly shorter wavelength, 416 nm, compared to the reduced state, and its intensity has increased ($\epsilon = 717$ mM$^{-1}$ cm$^{-1}$). These features are typical of CO binding to a ferrous *c*-type heme. There is also a shoulder present on the Soret band at a longer wavelength that indicates CO binding to a ferrous *b*-type heme. These changes are even more apparent in the reduced-CO *minus* reduced difference spectrum which clearly contains features associated with the binding of CO to both *c*- and *b*-type hemes (Figure 1B). Specifically, the maximum at 415 nm and a trough at 551 nm indicate binding of CO to a *c*-type heme, while a shoulder at ca. 424 nm and an inverted shoulder at 560 nm are typical of CO binding to a *b*-type heme, presumably heme $b_3$. The binding of CO to both heme $b_3$ and a single *c*-type heme is probably responsible for the broad asymmetric trough located in the Soret region at ca. 440 nm.

Saturation of a solution of fully reduced CcoP with CO elicited a number of changes in the electronic absorption spectrum (Figure 2A). Notably, the Soret maximum moved from 417 to 416 nm, and increased in intensity ($\epsilon = 316$ mM$^{-1}$ cm$^{-1}$). The reduced-CO *minus* reduced difference spectrum of CcoP (Figure 2B) contains a sharp derivative-shaped feature with a maximum at 415 nm and a minimum at ca. 428 nm as well as a trough in the visible region centered at 551 nm (Figure 2B). These features are all consistent with CO binding to ferrous *c*-type hemes. However, we noted that the spectral changes associated with CO binding were only fully developed when both hemes were completely reduced with dithionite. This is consistent with CO binding only to the *c*-type heme with the lower reduction potential, which we had previously determined to have bishistidine axial ligation.

*CO Binding to CcoP and Heme $b_3$.* Fully reduced cytochrome *cbb*$_3$ was titrated with CO and the extent of binding monitored at 415 nm, a wavelength chosen because it reports only the binding of CO to a *c*-type heme (Figure 3A). Fitting the experimental data yielded a dissociation constant ($K_d$) of $1.3 \times 10^{-6}$ M for the binding of CO to a single *c*-type heme in the holoenzyme. This value compares favorably with the experimentally determined value for the dissociation constant ($K_d = 2.2 \times 10^{-6}$ M) that describes the binding of CO to the bishistidine-coordinated *c*-type heme in isolated CcoP (Figure 3A). The similarity of these values suggests that CO binding to the active site heme $b_3$ does not compete with CO binding to CcoP in the cytochrome *cbb*$_3$ complex. We interpreted these observations in terms of a dissociation constant for CO binding to ferrous heme $b_3$ that is at least 1 order of magnitude greater than the constant for binding to CcoP.

The small change in absorbance associated with CO binding to reduced heme $b_3$ in the holoenzyme, together with the prediction of weaker binding, suggested that it was not appropriate to determine this dissociation constant in a static titration. Instead, the amplitude of the photolysis-induced absorbance change at 424 nm, a wavelength at which the $b_3$ heme contributes almost exclusively to the total absorbance change (see Figure 6), was determined over a range of CO concentrations (Figure 3B). These data yield a $K_d$ for CO binding to heme $b_3$ of $2.9 \times 10^{-5}$ M. The change in absorption due to photolysis measured at 415 nm, which only reports CO binding to *c*-type hemes, indicated that the CO-binding heme in CcoP was completely saturated at CO concentrations of 10 $\mu$M. This was true irrespective of whether CcoP was examined as an isolated subunit or as part of the cytochrome *cbb*$_3$ complex.

*Kinetics of CO Recombination to CcoP*. The transient absorption changes following photolysis of the CcoP−CO adduct are best described by two exponentials at all wavelengths and CO concentrations that we examined (Figure 4A). Although at lower (<200 $\mu$M) CO concentrations the contribution of the fast phase was difficult to deconvolute and was excluded from subsequent analysis, at 415 nm, at which the absorption change is largest in the static CO difference spectrum (Figure 2B), the fast (80% of the total absorbance change) and slow (20% of the total absorbance change) components had apparent rates of $9.1 \times 10^3$ and $1.7 \times 10^3$ s$^{-1}$, respectively, at a CO concentration of 1 mM. The total amplitude of this biphasic process was dependent on the wavelength used to monitor the reaction and closely followed the reduced *minus* reduced-CO difference spectrum obtained from equilibrium spectroscopic studies.

The fast ($\gamma_1$) and slow ($\gamma_2$) observed rate constants associated with CO recombination to isolated CcoP show an obvious dependency on CO concentration (Figure 4B,C) that was anticipated by Scheme 1. Simulation of these concentration dependencies using eqs 2 and 3 (Figure 4B,C) yields the three elemental rate constants ($k_H$, $k_{-H}$, and $k_{CO}$) presented in Table 1. Each of the three rate constants was calculated independently using $\gamma_1$ and $\gamma_2$, and the values are in good agreement with each other (Table 1). A time course simulated with the program Gepasi 3 (*26*−*28*) using the rate constants given in Table 1 closely approximates our experimental data for CO recombination to CcoP (Figure 5) and provides further evidence for the relevance of Scheme 1 to our experimental data.

*Kinetics of CO Recombination to Cytochrome cbb*$_3$. Since CO binds to both *c*- and *b*-type cytochromes, CO recombination to cytochrome *cbb*$_3$ oxidase was initially monitored at a series of wavelengths between 400 and 451 nm at 3 nm intervals. Inspection of the reaction time courses revealed that at particular wavelengths two processes identical in both rate and amplitude to those observed in isolated CcoP were present (see Figure 4 and Table 1). Consequently, these two components are attributed to CO recombination to CcoP as part of the cytochrome *cbb*$_3$ oxidase complex.

When the transient absorbance associated with CO recombination to CcoP is subtracted from the time courses recorded between 400 and 451 nm for the *cbb*$_3$ oxidase complex, it is possible to reconstruct, from the residual absorbance, a derivative-shaped kinetic difference spectrum (Figure 6A). This closely resembles the reduced-CO *minus* reduced difference spectrum resulting from CO binding to a

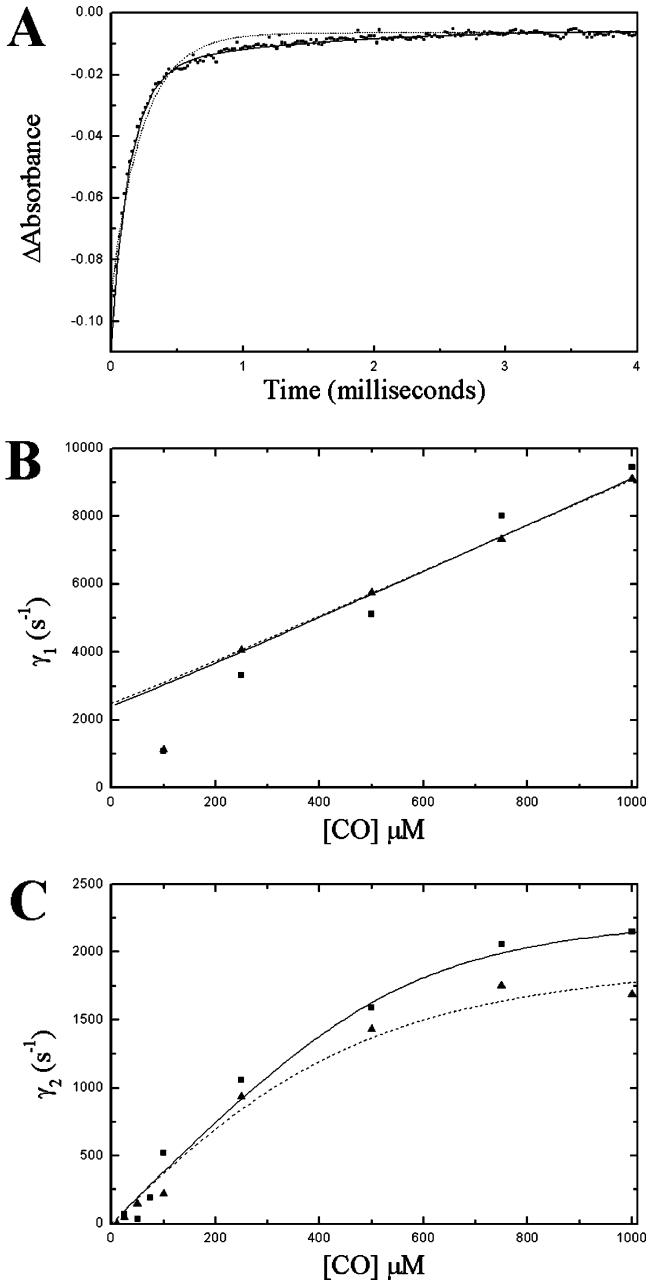


FIGURE 4: (A) Recombination of CO to isolated CcoP after photolysis (■) was monitored at 415 nm. The best fits to the experimental data using a single exponential (···) and the sum of two independent exponentials (—) are shown. The protein concentration was 4.6 $\mu$M in 20 mM sodium phosphate, 50 $\mu$M EDTA, and 0.02% (w/v) DM (pH 7.5), and the CO concentration was 1 mM. (B) Dependence upon CO concentration of the fast phase of recombination after photolysis to CcoP either as the isolated subunit (▲) or as a component of the cytochrome *cbb*$_3$ complex (■). Each data point represents an average of three separate experiments, each of which comprises the average of five to nine transients. The experimental data were fitted to eq 2 for both isolated CcoP (—) and the cytochrome *cbb*$_3$ complex (− − −). (C) Dependence upon CO concentration of the slow phase of recombination after photolysis to CcoP either as an isolated subunit (▲) or as a component of the cytochrome *cbb*$_3$ complex (■). Each data point represents an average of three separate experiments, each of which comprises the average of five to nine transients. The experimental data were fitted to eq 3 for both isolated CcoP (—) and the cytochrome *cbb*$_3$ complex (− − −).

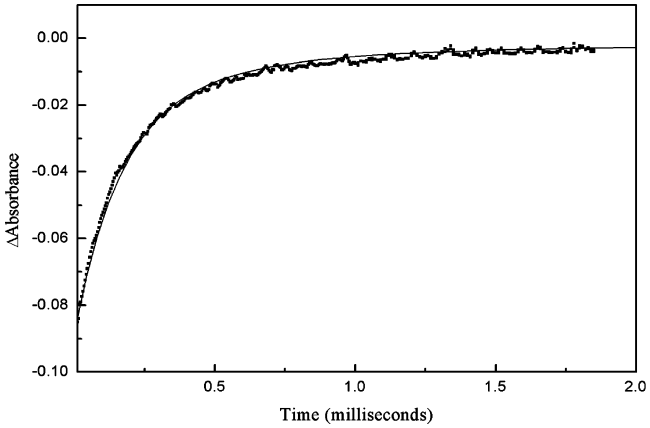


FIGURE 5: Recombination of reduced CcoP (4.6 $\mu$M) with CO (750 $\mu$M) after photolysis was monitored at 415 nm (■) in 20 mM sodium phosphate, 50 $\mu$M EDTA, and 0.02% (w/v) DM (pH 7.5). The time course of the reaction was simulated (—) with the program Gepasi 3 according to Scheme 1 using rate constants $k_H$, $k_{-H}$, and $k_{CO}$ given in Table 1.

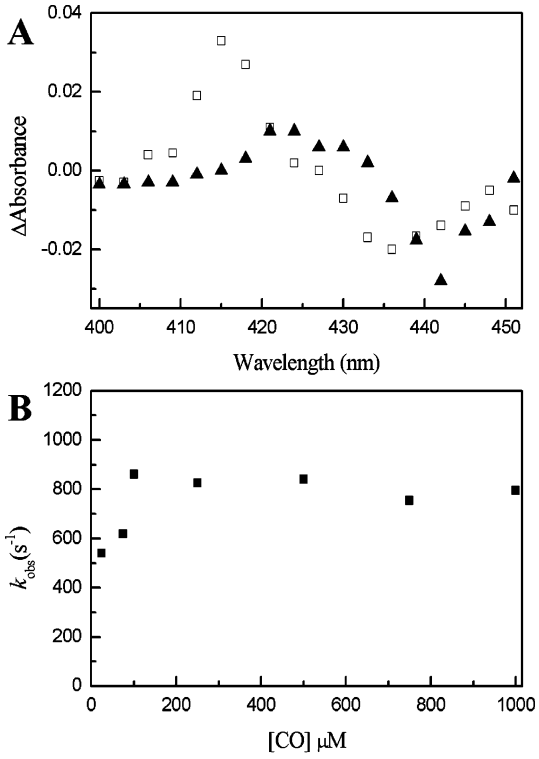


FIGURE 6: (A) Recombination of CO (1 mM) to cytochrome *cbb*$_3$ oxidase (2.5 $\mu$M) in 20 mM sodium phosphate, 50 $\mu$M EDTA, and 0.02% (w/v) DM (pH 7.5) was monitored at a series of wavelengths between 400 and 451 nm at 3 nm intervals. Each time course was analyzed in terms of three independent exponentials to take into account the biphasic reaction of CO with the reduced *c*-type heme, and the monophasic reaction with heme $b_3$. The total absorbance change associated with the two phases of CO recombination to the *c*-type heme (□) and the total absorbance change associated with the slowest phase assigned to CO recombination to heme $b_3$ (▲) were plotted as a function of wavelength. (B) Rate of CO recombination to heme $b_3$ after photolysis plotted as a function of CO concentration. Each data point represents an average of three separate experiments, each of which comprises the average of five to nine transients. The reaction was monitored at 424 nm, and the enzyme concentration was 2.3 $\mu$M in 20 mM sodium phosphate, 50 $\mu$M EDTA, and 0.02% (w/v) DM (pH 7.5).

ferrous *b*-type heme. Time courses measured at 424 nm, at which the absorption change associated with CO recombination to heme $b_3$ is largest but where there is no contribution from events at the *c*-type heme, can be described by a single exponential with an observed rate constant ($k_{obs}$) of 794 $s^{-1}$ which is not dependent upon CO concentration (Figure 6B).

Table 1: Summary of the Rate Constants Used in eqs 2−4 To Fit the Data Shown in Figures 5−8[a]

| | $k_{-H}$ ($s^{-1}$) | $k_H$ ($s^{-1}$) | $k_{CO}$ ($M^{-1}$ $s^{-1}$) |
|---|---|---|---|
| $\gamma_1$ (isolated CcoP) | 2198 | 294 | $6.8 \times 10^6$ |
| $\gamma_2$ (isolated CcoP) | 2117 | 617 | $5.0 \times 10^6$ |
| $\gamma_1$ (CcoP as part of cytochrome *cbb*$_3$) | 2152 | 250 | $6.9 \times 10^6$ |
| $\gamma_2$ (CcoP as part of cytochrome *cbb*$_3$) | 2394 | 251 | $4.3 \times 10^6$ |
| average | 2215 | 354 | $5.7 \times 10^6$ |
| rHb1 | 1911 | 517 | $6.0 \times 10^6$ |

[a] The equivalent rate constants for recombination of CO to reduced nonsymbiotic plant hemoglobin 1 (rHb1) are shown for comparison (*23*).

*Kinetics of the Initial Binding of CO to Reduced CcoP.* The initial reaction between reduced CcoP and CO was studied in rapid mixing experiments in which the concentration of CO was varied. The time course of this reaction at high CO concentrations (>25 $\mu$M) can be described in terms of a single-exponential process (Figure 7A). When the CO concentration was decreased to less than 25 $\mu$M, the reaction becomes distinctly biphasic (Figure 7B). Note that the single exponential observed at higher CO concentrations (>25 $\mu$M) corresponds to the slower of the two concentration-dependent processes observed at low CO concentrations. We presume that this is because at CO concentrations greater than 25 $\mu$M the fast phase is complete within the dead time of the stopped-flow spectrometer (~2 ms).

The rate constant that describes the fast process in these rapid mixing experiments clearly corresponds to $k_{CO}$, the rate of CO recombination to the pentacoordinate ferrous heme (P) in Scheme 1. However, Scheme 1 does not account for the slow process we observe at lower CO concentrations. As a consequence, we used the slightly more complex model outlined in Scheme 2 to account for our experimental data. This scheme proposes that in CcoP the ferrous *c*-type heme that binds CO exists in a mixture of ligation states prior to mixing with CO. Consequently, the slow phase of CO binding that we observe arises from that fraction of the protein ($H_C$) that must undergo conformational change to bind CO. Analysis of the dependence of the observed rate of this slow process upon CO concentration using eq 4 and constraining $k_{-H}$, $k_H$, and $k_{CO}$ to the values obtained from the flash photolysis experiments (Table 1) yields values of 200 and 350 $s^{-1}$ for $k_O$, and $k_{-O}$, respectively (Figure 8).

To ensure that Scheme 2 adequately describes the initial binding of CO to *c*-type heme in CcoP, we simulated the experimental time courses acquired by rapid mixing at high (Figure 7A) and low (Figure 7B) CO concentrations [simulated traces are depicted with the dashed lines (- - -)]. The first 2 ms was removed from the simulated time courses to take into account the absorbance changes that are lost during the dead time of mixing. The experimentally acquired and simulated data are in good agreement.

## DISCUSSION

*Spectroscopic Changes Associated with CO Binding to Cytochrome cbb*$_3$. The spectroscopic changes exhibited by reduced cytochrome *cbb*$_3$ oxidase in response to CO binding

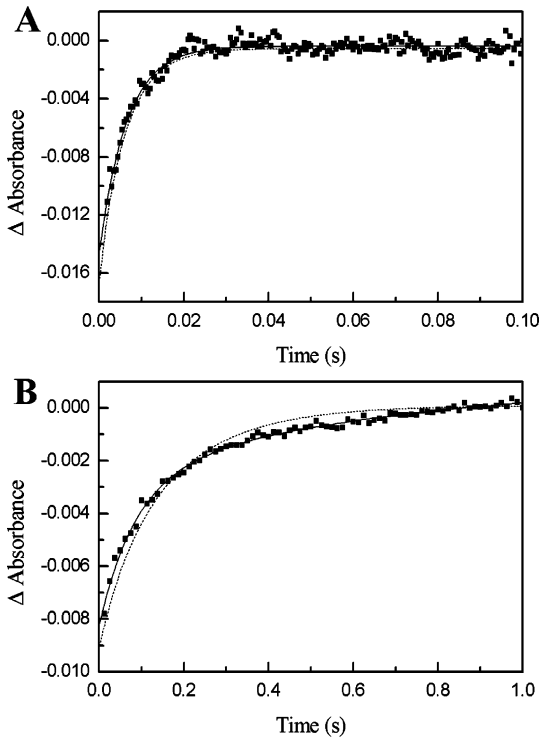


FIGURE 7: (A) Initial binding of CO (250 $\mu$M) to CcoP (1.1 $\mu$M) after rapid mixing in a stopped-flow spectrophotometer monitored at 415 nm (■). The experimental data were initially fitted using a single exponential (—). Subsequently, the time course of the reaction was simulated with the program Gepasi 3 according to Scheme 2 (···) using the previously determined values for $k_H$, $k_{-H}$, and $k_{CO}$ (Table 1) and values of 200 and 350 $s^{-1}$ for $k_O$ and $k_{-O}$, respectively. (B) Initial binding of CO (7.5 $\mu$M) to CcoP (1.1 $\mu$M) after rapid mixing in a stopped-flow spectrophotometer monitored at 415 nm (■). The experimental data were initially fitted using either a single exponential (— — —) or two independent exponentials (—). Subsequently, the time course of the reaction was simulated with the program Gepasi 3 according to Scheme 2 (···) using the previously determined values for $k_H$, $k_{-H}$, and $k_{CO}$ (Table 1) and values of 200 and 350 $s^{-1}$ for $k_O$ and $k_{-O}$, respectively. In both experiments, the reactions were carried out in 20 mM sodium phosphate, 50 $\mu$M EDTA, and 0.02% (w/v) DM (pH 7.5).

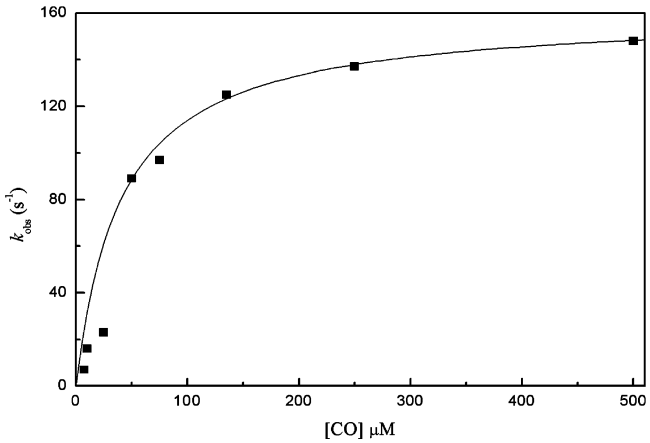


FIGURE 8: Concentration dependence of the observed rate constant for the slow phase of CO binding to CcoP in rapid mixing experiments. Each data point (■) is the average of two separate experiments, each of which comprises the average of five transients. The line is the best fit to the experimental data generated using eq 4 and constraining $k_H$, $k_{-H}$, and $k_{CO}$ to the values listed in Table 1, which yielded values of 200 and 350 $s^{-1}$ for $k_O$ and $k_{-O}$, respectively.

appear to be quite different from those reported for all other heme proteins, including other HCOs, with the single exception of bacterial NOR (*18*). For example, a derivative-shaped feature dominates the Soret region of the reduced-CO *minus* reduced difference spectrum of myoglobin, which contains a single *b*-type heme. The ratio between the maximum (421 nm) and the minimum (438 nm) of this derivative is 1.2:1. In contrast, the Soret region of the reduced-CO *minus* reduced difference spectrum of cytochrome *cbb*$_3$ is rather broader and much more complex, suggesting either that CO is displacing an endogenous ligand to heme $b_3$ or that it can also bind to a second heme. Earlier spectroscopic studies on periplasmic extracts that contained either overexpressed CcoO or CcoP indicated that only CcoP was capable of binding CO (*29*), and the data we present here are consistent with fully reduced CcoP binding CO stoichiometrically. Consequently, the form of the reduced-CO *minus* reduced difference spectrum of cytochrome *cbb*$_3$ is almost certainly a consequence of the overlapping features that result from CO binding to both *b*- and *c*-type hemes (see below).

There are inevitably some limitations to the accuracy of the kinetic difference spectrum (reduced-CO *minus* reduced) that we have determined for cytochrome *cbb*$_3$ oxidase. However, the contribution arising from CO recombination to CcoP is in good agreement with both the static and kinetic reduced-CO *minus* reduced difference spectra we have recorded for isolated CcoP. The peak at 424 nm in the kinetic CO difference spectrum corresponds to the shoulder at approximately the same wavelength in the static CO difference spectrum. Likewise, the broad asymmetric trough in the static CO difference spectrum of cytochrome *cbb*$_3$ oxidase can be explained in terms of overlapping features arising from CO binding to both heme types. It is possible that the considerable spectral overlap in the Soret region due to the contributions from CcoP and heme $b_3$ can account for some of the differences in the static CO difference spectra of cytochrome *cbb*$_3$ oxidase present in the literature. CcoP and heme $b_3$ have different affinities for CO. Consequently, if the CO adducts were prepared in different ways (for example, some may have been acquired by the addition of a small aliquot of CO while others may have been bubbled with CO for several minutes), the resultant spectra might represent different degrees of occupancy by CO at the two hemes.

Within the experimental error discussed above, it would appear that the static CO-difference spectrum and the kinetic difference spectrum regarding heme $b_3$ are in reasonable agreement. This suggests that heme $b_3$ becomes pentacoordinate upon reduction and accounts for its spectral similarities with postphotolysis heme $b_3$. This is consistent with evidence from resonance Raman spectroscopy that indicates that the $b_3$ is pentacoordinated in the reduced state (*30*).

*CO Binding to CcoP*. The pattern of kinetics of CO recombination to CcoP is similar to those seen in plant hemoglobins containing a hexacoordinated heme. This implies that CO binding must be preceded by displacement of an endogenous heme ligand. Several lines of evidence suggest that in the case of CcoP this is likely to be the distal histidine ligand, previously identified by NIR-MCD spectroscopy (*8*). First, CcoP must be fully reduced to allow complete formation of the CO adduct, suggesting that it is the heme with the lower potential (e.g., the bishistidine-coordinated heme) that binds CO. Second, when the me-

thionine residue, which provides the sixth axial ligand for cytochrome $c_{551}$ from *P. stutzeri*, is substituted with a histidine residue, by site-directed mutagenesis, CO is able to bind at neutral pH within seconds (*31*). Finally, the rate constants associated with binding of CO to CcoP are similar to those obtained for the replacement of an axial histidine ligand to the hexacoordinate heme in recombinant plant hemoglobin with CO (Table 1). It is noteworthy that the *E. coli* direct oxygen sensor (*Ec*Dos) protein also contains a hexacoordinate heme iron where it is a distal methionine ligand that is displaced by exogenous gaseous ligands rather than the proximal histidine ligand (*32*). However, the bimolecular rate constant for binding of CO to *Ec*Dos is extremely slow ($k_{on} = 1.1 \times 10^3$ $M^{-1}$ $s^{-1}$) (*33*).

The binding of gaseous ligands to the low-potential heme in CcoP appears then to be a competition between the binding of the exogenous ligand and endogeneous coordination by a local amino acid side chain. It is interesting to note that CO binding to a *c*-type cytochrome has also been reported in the *cbo*-type oxidase of *Methylobacillus flagellatus*, a member of the HCO superfamily that contains a *c*-type heme and heme O−$Cu_B$ dinuclear center (*34*). However, it is probably not a general characteristic of this family of enzymes, since there is no indication of CO ligation to the reduced heme C present in cytochrome $caa_3$ oxidase of *Bacillus subtilis* (*35*). Why should one of the hemes in CcoP bind a gaseous ligand such as CO? Previously, it was generally believed that only pentacoordinate ferrous heme could bind exogeneous ligands. However, recently, a new class of "heme-based sensors" involved in gene regulation have been described in which the heme iron is coordinated at both axial ligands by amino acid residues (*33*, *36*), one of which must be displaced by an exogenous ligand to allow its binding. Could it be that the binding of gaseous ligands to the low-potential heme of CcoP has a similar function?

There are a number of lines of circumstantial evidence to suggest that this might be the case. First, there is an apparent redundancy in the electron input strategy of cytochrome $cbb_3$ as highlighted by the observation that a subcomplex of the enzyme which lacks CcoP is catalytically competent (*9*, *10*). Second, in purple photosynthetic bacteria, CcoQ is proposed to mediate a signal that is generated by electron flow through cytochrome $cbb_3$ oxidase (*37*). The response to this signal is the repression of photosynthetic gene expression (*38*, *39*). However, CcoQ itself does not contain any redox active cofactors that could sense electron flow directly. Finally, the kinetics of CO recombination displayed by some plant hemoglobins, which contain a six-coordinate heme and are involved in physiological stress responses such as hypoxia, are very similar to those we report for CcoP. These arguments are also consistent with the view expressed in a recent review by Myllykallio and Liebl (*40*) that the absence of oxidative stress regulators such as OxyR, SoxR, and SoxS in *Helicobacter pylori* could suggest that cytochrome $cbb_3$ might directly sense environmental changes and transduce the signal. Recall that cytochrome $cbb_3$ is the only terminal oxidase in this organism.

Since CO is a substrate analogue of NO and $O_2$, it has found wide application as a molecular probe of hemes in sensory domains that respond to these two physiologically important ligands. There are also examples of heme-based sensors that specifically respond to CO in both prokaryotes and eukaryotes (*36*, *41*). All heme-based gas sensors described to date contain *b*-type heme in their sensory domains. However, the recently reported X-ray structure of SHP (*sphaeroides* heme protein), a 12 kDa oxygen binding cytochrome *c* from *Rhodobacter sphaeroides*, suggests that this may not be universally true (*42*). In the oxidized state, the single *c*-type heme of SHP is hexacoordinate, with histidine and asparagine as axial ligands. On reduction, the heme sheds the distal asparagine ligand and can readily bind CO ($K_d = 3.3 \times 10^{-5}$ M) (*43*). The simple kinetics of association of CO with this pentacoordinate heme are quite slow, unlike the complex CO binding kinetics exhibited by CcoP. Reduced SHP also binds oxygen transiently, but the heme readily autoxidizes ($t_{1/2} \sim 3$ min), a property that is rather reminiscent of the gas-sensing heme of FixL rather than an oxygen binding pigment such as myoglobin (*44*).

It is hard to envisage a requirement for CO sensing in *P. stutzeri*. However, if the low-potential heme of CcoP could bind either oxygen or NO it could, in principle, provide a mechanism for reporting the environmental concentrations of these gases and moderating the activity of the $cbb_3$ oxidase complex.

*Binding of CO to Heme $b_3$*. The process of CO binding to the active site of cytochrome $cbb_3$ oxidase, as identified here, is also worthy of comment. HCOs typically have bimolecular rate constants for CO recombination of $6-10 \times 10^4$ $M^{-1}$ $s^{-1}$ with off rates of $<1$ $s^{-1}$ and as a result an equilibrium dissociation constant of ca. $1 \times 10^6$ M (*13*, *35*, *45*). Thus, the results reported here concerning the rate of interaction of CO and heme $b_3$ were unexpected. It has recently been demonstrated by time-resolved room-temperature FTIR spectroscopy that in contrast to other HCOs the transient decay of the $Cu_B$−CO complex in cytochrome $cbb_3$ oxidase of *P. stutzeri* is concurrent with the formation of the Fe(II)−CO complex (*46*). Moreover, Stavrakis and colleagues (*46*) found no evidence that CO escapes from the dinuclear center. Their findings are consistent with the concentration-independent rate of CO recombination reported here. Furthermore, the rates reported here (ca. 800 $s^{-1}$) for the formation of the $b_3$−CO complex and by Stavrakis and colleagues (*46*) (ca. $5 \times 10^3$ $s^{-1}$) for the transfer of CO from $Cu_B$ to $b_3$ are in reasonable agreement, considering the different experimental setups.

The origin of this rather unusual reactivity of the active site of $cbb_3$ toward CO is not certain, but it undoubtedly reflects other properties of cytochrome $cbb_3$ that are markedly different from those of the well-characterized bacterial HCOs, cytochrome $aa_3$ and cytochrome $bo_3$. Recall that $cbb_3$ oxidases apparently have a high affinity for oxygen [$k_m \sim 7$ nM (*3*)] but retain the ability to pump protons (*4*). In addition, many of the ionizable residues that form two structurally defined channels, known as the D- and K-channels, that facilitate proton transport from the cytoplasm to the buried dinuclear center during turnover in cytochrome $aa_3$ are absent in the derived amino acid sequence of CcoN (*7*, *9*). Notably, $cbb_3$-type oxidases lack a homologue of Tyr280 (the residue numbering corresponds to the *Pseudomonas denitrificans* cytochrome $aa_3$ sequence), which is covalently attached to His284 in the $aa_3$ oxidase (*47*) forming a site capable of stabilizing a radical species during oxygen reduction (*48*). The absence of this His/Tyr pair in the $cbb_3$-type oxidases and the presence of a *b*-type heme may contribute to a very

differently organized dinuclear center in which exchange of CO between $Cu_B$ and heme $b_3$ is significantly enhanced. This may reflect an important determinant of substrate affinity.

## CONCLUSIONS

The work described here establishes that there is a clear difference between the interaction of CO with the active site of cytochrome *cbb*$_3$ oxidases and other HCOs. It also establishes that CO binds to CcoP as well as heme $b_3$. The mechanism of CO combination to CcoP appears to be similar to that observed in a hexacoordinate plant hemoglobin (*23*). The interaction between cytochrome *cbb*$_3$ oxidase and CO is complex, and it appears that this reactivity may not only provide insight into the nature of the ligand capture by the active site of cytochrome *cbb*$_3$ oxidase but also indicate a sensing function for CcoP.

## ACKNOWLEDGMENT

We thank David Clarke and Jeremy Thornton for their help with culturing cells and protein purification. Expression of recombinant CcoP would not have been possible without the plasmid pEC86 which was a kind gift of Dr. Linda Thöny-Meyer (ETH, Zurich, Switzerland).

## REFERENCES

1. van der Oost, J., deBoer, A. P. N., deGier, J.-W. L., Zumft, W. G., Stouthamer, A. H., and van Spanning, R. J. M. (1994) *FEMS Microbiol. Lett. 121*, 1−9.
2. Saraste, M., and Castresana, J. (1994) *FEBS Lett. 341*, 1−4.
3. Preisig, O., Zufferey, R., Thöny-Meyer, L., Appleby, C. A., and Hennecke, H. (1996) *J. Bacteriol. 178*, 1532−1538.
4. Raitio, M., and Wikström, M. (1994) *Biochim. Biophys. Acta 1186*, 100−106.
5. Pitcher, R. S., Brittain, T., and Watmough, N. J. (2002) *Biochem. Soc. Trans. 30*, 653−658.
6. Preisig, O., Anthamatten, D., and Hennecke, H. (1993) *Proc. Natl. Acad. Sci. U.S.A. 90*, 3309−3313.
7. Pereira, M. M., Santana, M., and Teixeira, M. (2001) *Biochim. Biophys. Acta 1505*, 185−208.
8. Pitcher, R. S., Cheesman, M. R., and Watmough, N. J. (2002) *J. Biol. Chem. 277*, 31474−31483.
9. de Gier, J.-W. L., Schepper, M., Reijnders, W. N. M., van Dyck, S. J., Slotboom, D. J., Warne, A., Saraste, M., Krab, K., Finel, M., Stouthamer, A. H., van Spanning, R. J. M., and van der Oost, J. (1996) *Mol. Microbiol. 20*, 1247−1260.
10. Zufferey, R., Preisig, O., Hennecke, H., and Thöny-Meyer, L. (1996) *J. Biol. Chem. 271*, 9114−9119.
11. Pitcher, R. S. (2002) Biochemical and Spectroscopic Studies of Cytochrome *cbb*$_3$ Oxidase from *Pseudomonas stutzeri*, Ph.D. Thesis, University of East Anglia, Norwich, U.K.
12. Wood, P. M. (1984) *Biochim. Biophys. Acta 768*, 293−317.
13. Gibson, Q. H., and Greenwood, C. (1963) *Biochem. J. 86*, 541−554.
14. Springer, B. A., Sligar, S. G., Olson, J. S., and Phillips, G. N. (1994) *Chem. Rev. 94*, 699−714.
15. Einarsdóttir, O., Dyer, R. B., Lemon, D. D., Killough, P. M., Hubig, S. M., Atherton, S. J., López-Garriga, J. J., Palmer, G., and Woodruff, W. H. (1993) *Biochemistry 32*, 12013−12024.
16. Lemon, D. D., Calhoun, M. W., Gennis, R. B., and Woodruff, W. H. (1993) *Biochemistry 32*, 11953−11956.
17. Fiamingo, F. G., Altschuld, R. A., Moh, P. P., and Alben, J. O. (1982) *J. Biol. Chem. 257*, 1639−1650.
18. Hendriks, J. H., Prior, L., Baker, A. R., Thomson, A. J., Saraste, M., and Watmough, N. J. (2001) *Biochemistry 40*, 13361−13369.
19. Hendriks, J., Warne, A., Gohlke, U., Haltia, T., Ludovici, C., Lubben, M., and Saraste, M. (1998) *Biochemistry 37*, 13102−13109.
20. Ädelroth, P., Brzezinski, P., and Malmström, B. G. (1995) *Biochemistry 34*, 2844−2849.
21. Keefe, R. G., and Maier, R. J. (1993) *Biochim. Biophys. Acta 1183*, 91−104.
22. Berry, E. A., and Trumpower, B. L. (1987) *Anal. Biochem. 161*, 1−15.
23. Hargrove, M. S. (2000) *Biophys. J. 79*, 2733−2738.
24. Capellos, C., and Bielski, B. (1972) *Kinetic Systems*, John Wiley and Sons, New York.
25. Trent, J. T., III, Hvitved, A. N., and Hargrove, M. S. (2001) *Biochemistry 40*, 6155−6163.
26. Mendes, P. (1993) *Comput. Appl. Biosci. 9*, 563−571.
27. Mendes, P. (1997) *Trends Biochem. Sci. 22*, 361−363.
28. Mendes, P., and Kell, D. (1998) *Bioinformatics 14*, 869−883.
29. Arslan, E., Schulz, H., Zufferey, R., Kunzler, P., and Thony-Meyer, L. (1998) *Biochem. Biophys. Res. Commun. 251*, 744−747.
30. Varotsis, C., Babcock, G. T., Garcia-Horsman, J. A., and Gennis, R. B. (1995) *J. Phys. Chem. 99*, 16817−16820.
31. Miller, G. T., Zhang, B., Hardman, J. K., and Timkovich, R. (2000) *Biochemistry 39*, 9010−9017.
32. Gonzalez, G., Dioum, E. M., Bertolucci, C. M., Tomita, T., Ikeda-Saito, M., Cheesman, M. R., Watmough, N. J., and Gilles-Gonzalez, M. A. (2002) *Biochemistry 41*, 8414−8421.
33. Delgado-Nixon, V. M., Gonzalez, G., and Gilles-Gonzalez, M. A. (2000) *Biochemistry 39*, 2685−2691.
34. Strom, E. V., Dinarieva, T. Y., and Netrusov, A. I. (2001) *FEBS Lett. 505*, 109−112.
35. Hill, B. C. (1996) *Biochemistry 35*, 6136−6143.
36. Lanzilotta, W. N., Schuller, D. J., Thorsteinsson, M. V., Kerby, R. L., Roberts, G. P., and Poulos, T. L. (2000) *Nat. Struct. Biol. 7*, 876−880.
37. Oh, J. I., and Kaplan, S. (1999) *Biochemistry 38*, 2688−2696.
38. O'Gara, J. P., Eraso, J. M., and Kaplan, S. (1998) *J. Bacteriol. 180*, 4044−4050.
39. Oh, J. I., and Kaplan, S. (2000) *EMBO J. 19*, 4237−4247.
40. Myllykallio, H., and Liebl, U. (2000) *Trends Microbiol. 8*, 542−543.
41. Dioum, E. M., Rutter, J., Tuckerman, J. R., Gonzalez, G., Gilles-Gonzalez, M. A., and McKnight, S. L. (2002) *Science 298*, 2385−2387.
42. Leys, D., Backers, K., Meyer, T. E., Hagen, W. R., Cusanovich, M. A., and Van Beeumen, J. J. (2000) *J. Biol. Chem. 275*, 16050−16056.
43. Klarskov, K., Van Driessche, G., Backers, K., Dumortier, C., Meyer, T. E., Tollin, G., Cusanovich, M. A., and Van Beeumen, J. J. (1998) *Biochemistry 37*, 5995−6002.
44. Gilles-Gonzalez, M. A., Gonzalez, G., Perutz, M. F., Kiger, L., Marden, M. C., and Poyart, C. (1994) *Biochemistry 33*, 8067−8073.
45. Cheesman, M. R., Watmough, N. J., Pires, C. A., Turner, R., Brittain, T., Gennis, R. B., Greenwood, C., and Thomson, A. J. (1993) *Biochem. J. 289*, 709−718.
46. Stavrakis, S., Koutsoupakis, K., Pinakoulaki, E., Urbani, A., Saraste, M., and Varotsis, C. (2002) *J. Am. Chem. Soc. 124*, 3814−3815.
47. Ostermeier, C., Harrenga, A., Ermler, U., and Michel, H. (1997) *Proc. Natl. Acad. Sci. U.S.A. 94*, 10547−10553.
48. Gennis, R. B. (1998) *Biochim. Biophys. Acta 1365*, 241−248.

BI0343469